



Dipole-Scattering by Spherical Media and Related Optimization Problems

Zoi Tsitsoglu, Prokopios Prokopiou, and Nikolaos L. Tsitsas*

School of Informatics, Aristotle University of Thessaloniki, Thessaloniki 54124, Greece

Abstract

A layered spherical medium is excited by an arbitrary internal or external dipole. Direct scattering problems are investigated analytically by employing a dyadic Green's function technique. Inverse scattering problems concerning the determination of the medium's parameters are subsequently considered in the low-frequency regime. Specific optimization problems are examined, referring to the determination of the medium's parameters so that the far-field exhibits desired variations. Certain initial numerical results on such problems are presented.

1. Introduction

A point-dipole radiating in the interior of a spherical medium provides an approximate but realistic model in antennas implantations inside the head for hyperthermia or biotelemetry [1] as well as in several biomedical imaging applications, including e.g. brain medical imaging [2], [3], electroencephalography [4], magnetoencephalography [5], and magnetic resonance imaging [6]. External dipole excitation of a sphere can model effectively the interaction between the mobile phone antenna and the human head [7].

In this work, we investigate the electromagnetic excitation of a layered sphere by an arbitrary dipole located inside or outside the sphere. The exact dyadic Green's function is determined by analytical techniques. Asymptotic approximations of the far-field patterns in the low-frequency regime are subsequently obtained. Far-field *inverse medium* scattering algorithms are established concerning the determination of the scatterer's material parameters. These algorithms use measurements of the different orders of the far-field patterns expansions at certain observation angles.

Furthermore, the exact solutions of the direct scattering problem can be exploited as suitable objective functions in optimization problems concerning the determination of the layers radii, permittivities and permeabilities so that the far-field patterns exhibit desired characteristics. Aspects of this type of problems have been investigated in [8]-[10] mainly for problems of cloaking a spherical object under plane-wave incidence. Here, we present certain initial numerical optimization results for the

reduction in the backscattering cross section of a sphere covered by a suitable number of layers.

The $\exp(-i\omega t)$ time dependence is assumed and suppressed throughout, where ω is the angular frequency.

2. Direct Scattering Problem

A layered spherical medium V with radius a_1 is excited by an arbitrary internal or external electric dipole. The interior of V is divided by $P-1$ concentric spheres $r=a_p$ ($p=2,\dots,P$) into $P-1$ homogeneous dielectric layers V_p ($p=1,\dots,P-1$), consisting of materials with dielectric permittivities ε_p and magnetic permeabilities μ_p , and surrounding a perfect electric conducting (PEC) core (layer V_P). The exterior V_0 of V is an infinite homogeneous medium with permittivity ε_0 and permeability μ_0 . The infinitesimal electric dipole with dipole moment \mathbf{p} , located at $\mathbf{r}_q=(r_q, \theta_q, \phi_q)$ of layer V_q ($q=0,\dots,P$), generates at $\mathbf{r}=(r, \theta, \phi)$ (with $\mathbf{r} \neq \mathbf{r}_q$) the primary electric field

$$\mathbf{E}^{\text{pr}}(\mathbf{r}; \mathbf{r}_q, \mathbf{p}) = i \omega \mu_q \tilde{\mathbf{G}}^{\text{pr}}(\mathbf{r}; \mathbf{r}_q) \cdot \mathbf{p}, \quad (1)$$

where $\tilde{\mathbf{G}}^{\text{pr}}$ is the primary dyadic Green's function, i.e. the dyadic Green's function corresponding to the contribution of the dipole in the infinite homogeneous space filled by the material of V_q .

The exact Green's function of the layered spherical scatterer can be determined analytically as follows. According to the scattering superposition method [11], the total electric Green's function in the dipole's layer V_q assumes the decomposition

$$\tilde{\mathbf{G}}^q(\mathbf{r}, \mathbf{r}') = \tilde{\mathbf{G}}^{\text{pr}}(\mathbf{r}, \mathbf{r}') + \tilde{\mathbf{G}}^{\text{sec}}(\mathbf{r}, \mathbf{r}'), \quad \mathbf{r}, \mathbf{r}' \in V_q, \quad \mathbf{r} \neq \mathbf{r}', \quad (2)$$

where the secondary component $\tilde{\mathbf{G}}^{\text{sec}}$ of the Green's function is due to scattering by the boundaries of the spherical shells. The primary and secondary components are expressed as series of the spherical vector wave functions. More precisely, the known primary component is expressed by (10.24) of [11] (see also [12]), while the unknown secondary components in the spherical shells V_p ($p=1,\dots,P, p \neq q$) are expressed as

$$\begin{aligned} \tilde{\mathbf{G}}^p(\mathbf{r}, \mathbf{r}') = & \frac{i k_q}{4\pi} \sum_{n=1}^{\infty} \sum_{m=0}^n \sum_{\sigma=e,o} \frac{2n+1}{n(n+1)} \varepsilon_m \frac{(n-m)!}{(n+m)!} \times \\ & \left\{ \mathbf{M}_{\sigma mn}^1(\mathbf{r}, k_p) \left[\alpha_n^{pq} \mathbf{M}_{\sigma mn}^1(\mathbf{r}', k_q) + \beta_n^{pq} \mathbf{M}_{\sigma mn}^3(\mathbf{r}', k_q) \right] + \right. \\ & \mathbf{N}_{\sigma mn}^1(\mathbf{r}, k_p) \left[\gamma_n^{pq} \mathbf{N}_{\sigma mn}^1(\mathbf{r}', k_q) + \delta_n^{pq} \mathbf{N}_{\sigma mn}^3(\mathbf{r}', k_q) \right] + \\ & \mathbf{M}_{\sigma mn}^3(\mathbf{r}, k_p) \left[\tilde{\alpha}_n^{pq} \mathbf{M}_{\sigma mn}^1(\mathbf{r}', k_q) + \tilde{\beta}_n^{pq} \mathbf{M}_{\sigma mn}^3(\mathbf{r}', k_q) \right] + \\ & \left. \mathbf{N}_{\sigma mn}^3(\mathbf{r}, k_p) \left[\tilde{\gamma}_n^{pq} \mathbf{N}_{\sigma mn}^1(\mathbf{r}', k_q) + \tilde{\delta}_n^{pq} \mathbf{N}_{\sigma mn}^3(\mathbf{r}', k_q) \right] \right\}, \end{aligned} \quad (3)$$

where the involved spherical vector wave functions are defined according to (10.9) and (10.10) of [11], while $\varepsilon_m = 1$ for $m=0$ and 2 for $m \neq 0$, and k_p denotes the wavenumber of layer V_p . The uniform convergence of the series (3) was described in [13] by following the analysis of [14]. The unknown coefficients in the secondary components expansions (3) are determined analytically by imposing the transmission boundary conditions on the interfaces of the spherical shells and applying a *T-matrix method*, as described in detail in [15]. Then, the electric field generated in any shell V_p by the arbitrary electric dipole located in shell V_q is given by

$$\mathbf{E}^p(\mathbf{r}; \mathbf{r}_q, \mathbf{p}) = i \omega \mu_p \tilde{\mathbf{G}}^p(\mathbf{r}; \mathbf{r}_q) \cdot \mathbf{p}, \quad \mathbf{r} \in V_p. \quad (4)$$

Moreover, by using the asymptotic expressions of the spherical vector wave functions [15], we get the exact expressions of the electric far-field pattern \mathbf{g} , which is defined by

$$\mathbf{E}^0(\mathbf{r}; \mathbf{r}_q, \mathbf{p}) = \mathbf{g}(\mathbf{r}; \mathbf{r}_q, \mathbf{p}) h_0(k_0 r) + O(r^{-2}), \quad r \rightarrow \infty, \quad (5)$$

where h_0 is the zero-th order spherical Hankel function of the first kind.

3. Inverse Scattering Algorithms

The exact far-field patterns, determined by the procedure described in Section 2 above, are difficult to be processed in order to develop inverse scattering algorithms, referring to the determination of the characteristics of the spherical medium. However, under the low-frequency assumption $k_0 a_1 \ll 1$, i.e. by assuming that the scatterer's external radius a_1 is much smaller than the primary field's wavelength, we may obtain simplified expressions of the far-field patterns, which can be worked out in the framework of inverse scattering algorithms. The low-frequency assumption is realistic in relevant applications, like e.g. in medical imaging applications, where $k_0 a_1$ is usually of the order of 10^{-7} [16].

The aforementioned simplified expansions of the far-field patterns in the low-frequency region are derived in [15] by using the small-arguments asymptotic expressions of the spherical Bessel and Hankel functions. These expansions will form the basis for the development of *inverse medium algorithms*, concerning the determination of a homogeneous sphere's material parameters. The

essential idea in such algorithms is to measure different orders of the far-fields expansions at certain observation angles and combine the measurements to derive a single equation for each unknown parameter (inverse algorithms of this type in acoustics were developed in [17]).

More precisely, in our setting, we will determine the relative dielectric permittivity ε_r and magnetic permeability μ_r of a homogeneous dielectric spherical medium by using two far-field measurements for certain specific locations and polarizations of an external low-frequency dipole. The known quantities are the sphere's radius a_1 and center, the external dipole's parameters as well as the parameters ε_0 and μ_0 of the exterior region. First, we measure the leading-order term m_1 of the φ -component of the far-field pattern, at the observation angles $(\theta, \varphi) = (\pi/2, 0)$ for a x -polarized external dipole located at $(r_0, \theta_0, \varphi_0) = (b, \pi/2, \pi/4)$, where $b > a_1$ is a known chosen fixed length. Then, the sphere's relative permittivity is determined as

$$\varepsilon_r = \frac{3a_1^3 + 4b^3 m_1}{3a_1^3 - 2b^3 m_1}. \quad (6)$$

Next, we measure the second-order term m_2 of the θ -component of the far-field pattern, at the observation angles $(\theta, \varphi) = (\pi/2, 0)$ for a z -polarized external dipole located at $(r_0, \theta_0, \varphi_0) = (b, \pi/2, 0)$, yielding the sphere's relative permeability as

$$\mu_r = \frac{a_1^2 + 2b^2 m_2}{a_1^2 - b^2 m_2}. \quad (7)$$

The above described far-field inverse medium algorithm can be realized experimentally in an entirely non-invasive way, since it does not involve measurements due to internal dipoles.

4. Optimization Problems

The derived solutions of the direct scattering problem will be now utilized in order to examine certain optimization problems, referring to the design of a layered spherical medium, exhibiting desired far-field characteristics. To this end, we consider the expression of the *bistatic (differential) scattering cross section*

$$\sigma(\theta, \varphi; \mathbf{r}_0) = \frac{4\pi}{k_0^2} \left[|S_\theta(\theta; \mathbf{r}_0)|^2 \cos^2 \varphi + |S_\varphi(\theta; \mathbf{r}_0)|^2 \sin^2 \varphi \right], \quad (8)$$

referring to a y -polarized external dipole located on the z -axis, where functions S_θ and S_φ are defined in [18]. The objective function we will consider in the following optimization schemes is the *normalized backscattering cross section* $\sigma(0; \mathbf{r}_0)/(\pi a_1^2)$, which is usually the basic quantity to be minimized in practical applications.

An optimization methodology based on the *Particle Swarm Optimization (PSO)* was developed for the minimization of this objective function. The considered optimization variables were the permittivities, the permeabilities as well as the radii of the $P-1$ layers covering the PEC core. The radius of the PEC core was fixed at one free-space wavelength, namely $k_0 a_p = 2\pi$. The distance r_0 of the dipole's position was taken such that $k_0 r_0 \geq 15$ in which case the dipole's spherical incident field approximates the respective plane wave, and hence the obtained far-field results are close to those of the plane-wave incidence problem; the related numerical analysis justifying this estimation is included in [18].

The obtained optimized values of the normalized backscattering cross section versus the number of layers covering the PEC core are depicted in Fig. 1. It is observed that for each number of covering layers an optimized solution was found yielding a reduction in the examined objective function. This reduction is significant (e.g. under a threshold of 10 dB) in the cases of 1, 3, 5, 6, and 10 layers covering the PEC core.

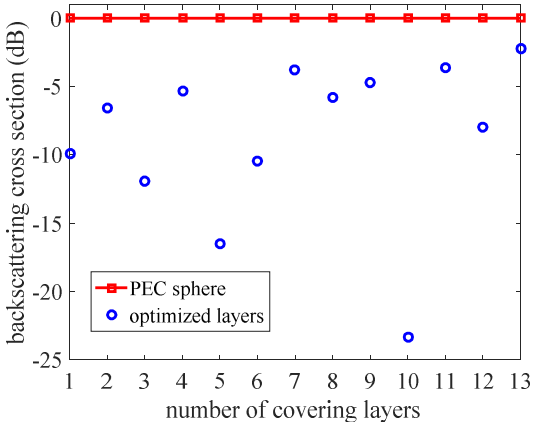


Figure 1. Optimized values of the normalized backscattering cross section $\sigma(0; \mathbf{r}_0)/(\pi a_1^2)$, as obtained by the developed PSO algorithm, versus the number of layers covering the PEC core.

The obtained results for the optimized layers (presented in Fig. 1), offering reduced backscattering cross section, are now tested with respect to their variations for different angles of observation. To this direction, some representative numerical results for one and ten covering layers are depicted in Fig. 2, showing the normalized bistatic scattering cross section $\sigma(\theta, \varphi; \mathbf{r}_0)/(\pi a_1^2)$ as function of the angle θ in the xOz and yOz planes. The PEC sphere covered with the determined optimized ten dielectric layers exhibits reduced scattering cross section with respect to the bare PEC sphere not only for a narrow region in the backscattering regime (for which the configuration was originally optimized), but also most of the observation angles up to the xOy plane (i.e. for θ up to 90°)

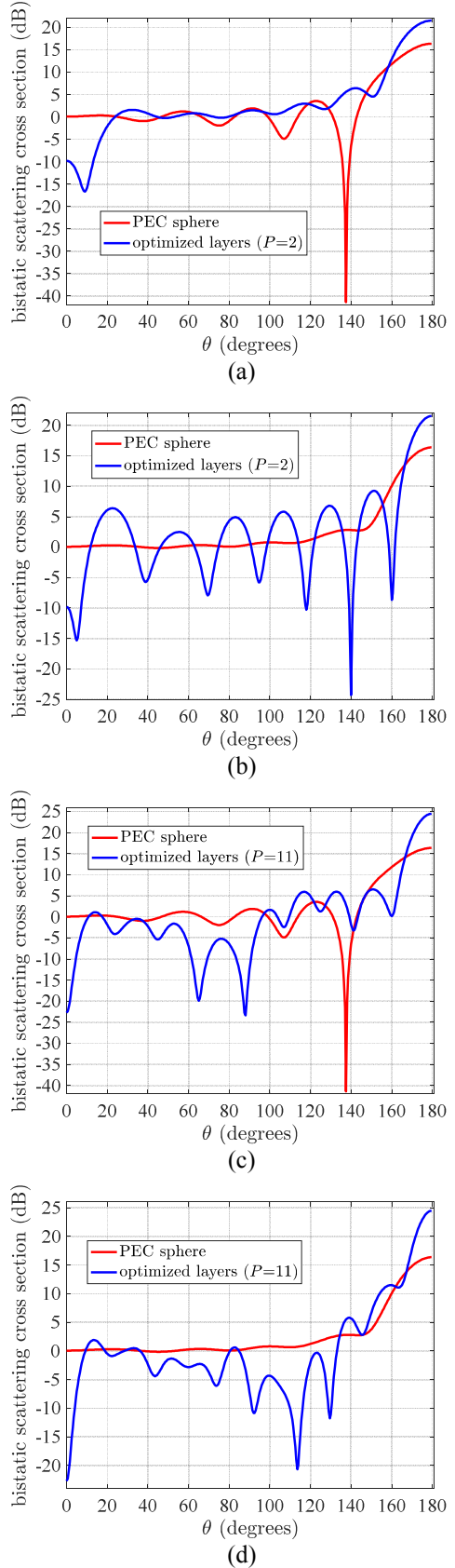


Figure 2. Normalized bistatic cross section versus the observation angle θ for one and ten covering layers with parameters computed by the PSO algorithm (c.f. Fig. 1); (a), (c) refer to the xOz plane and (b), (d) to the yOz plane.

Additional numerical results have been computed and will be presented at the conference. Particularly, optimizations of the backscattering cross section for a dipole in close proximity to the spherical medium and the variations of the results with respect to the dipole's distance from the sphere's center will be analyzed.

5. References

1. J. Kim and Y. Rahmat-Samii, "Implanted antennas inside a human body: simulations, designs, and characterizations," *IEEE Trans. Microw. Theory Tech.*, **52**, 2004, pp. 1934-1943.
2. G. Dassios, "Electric and magnetic activity of the brain in spherical and ellipsoidal geometry," *Lecture Notes Math.*, **1983**, 2009, pp. 133-202.
3. H. Ammari, *An Introduction to Mathematics of Emerging Biomedical Imaging*, Springer, Berlin, 2008.
4. J. J. Riera, M. E. Fuentes, P. A. Valdés, and Y. Ohárriz, "EEG-distributed inverse solutions for a spherical head model," *Inverse Problems*, **14**, 1998, pp. 1009-1019.
5. A. S. Fokas, "Electromagneto-encephalography for a three-shell model: distributed current in arbitrary, spherical and ellipsoidal geometries," *J. Royal Soc. Interface*, **6**, 2009, pp. 479-488.
6. F. Liu and S. Crozier, "Electromagnetic fields inside a lossy, multilayered spherical head phantom excited by MRI coils: models and methods," *Phys. Med. Biol.*, **49**, 2004, pp. 1835-1851.
7. M. Okoniewski and M. A. Stuchly, "A study of the handset antenna and human body interaction," *IEEE Trans. Microwave Theory Tech.*, **44**, 1996, pp. 1855-1864.
8. C.-W. Qiu, L. Hu, B. Zhang, B.-I. Wu, S. G. Johnson, and J. D. Joannopoulos, "Spherical cloaking using nonlinear transformations for improved segmentation into concentric isotropic coatings," *Optics Express*, **17**, 2009, pp. 13467-13478.
9. G. Castaldi, I. Gallina, V. Galdi, A. Alù, and N. Engheta, "Analytical study of spherical cloak/anti-cloak interactions," *Wave Motion*, **48**, 2011, pp. 455-467.
10. T. C. Martins and V. Dmitriev, "Spherical invisibility cloak with minimum number of layers of isotropic materials," *Microwave Opt. Technol. Letters*, **54**, 2012, pp. 2217-2220.
11. C.-T. Tai, *Dyadic Green Functions in Electromagnetic Theory*, IEEE Press, 1994.
12. L.-W. Li, P.-S. Kooi, M. S. Leong, and T.-S. Yeo, "Electromagnetic Dyadic Green's Function in Spherically Multilayered Media," *IEEE Trans. Microwave Theory and Techniques*, **42**, 1994, pp. 2302-2310.
13. N. L. Tsitsas, "Direct and inverse dipole electromagnetic scattering by a piecewise homogeneous sphere," *Zeitschrift für Angewandte Mathematik und Mechanik (ZAMM)*, **89**, 2009, pp. 833-849.
14. K. Aydin and A. Hizal, "On the Completeness of the Spherical Vector Wave Functions," *J. Math. Anal. Appl.*, **117**, 1986, pp. 428-440.
15. P. Prokopiou and N. L. Tsitsas, Electromagnetic Excitation of a Spherical Medium by an Arbitrary Dipole and Related Inverse Problems, *Studies in Applied Mathematics*, in press, 2018.
16. N. L. Tsitsas and P. A. Martin, "Finding a source inside a sphere," *Inverse Problems*, **28**, 2012, 015003.
17. P. Prokopiou and N. L. Tsitsas, "Direct and inverse low-frequency acoustic excitation of a layered sphere by an arbitrarily positioned point source," *Math. Methods Appl. Sci.*, **41**, 2018, 1040-1046.
18. N. L. Tsitsas and C. Athanasiadis, "On the scattering of spherical electromagnetic waves by a layered sphere," *Quart. J. Mech. Appl. Math.*, **59**, 2006, 55-74.